PROCEEDINGS OF SCIENCE

Comparison of lattice QCD+QED predictions for radiative leptonic decays of light mesons with experimental data

R. Frezzotti,[a] **M. Garofalo,**[b] **V. Lubicz,**[c] **G. Martinelli,**[d] **C.T. Sachrajda,**[e] **F. Sanfilippo,**[f] **S. Simula**[f,*] **and N. Tantalo**[a]

[a] *Dipartimento di Fisica and INFN, Università di Roma "Tor Vergata", I-00133 Rome, Italy*
[b] *HISKP (Theory), Rheinische Friedrich-Wilhelms-Universität Bonn, Germany*
[c] *Dipartimento di Matematica e Fisica and INFN, Università di Roma Tre, I-00146 Rome, Italy*
[d] *Dipartimento di Fisica and INFN, Università di Roma "La Sapienza", I-00185 Rome, Italy*
[e] *Department of Physics and Astronomy, University of Southampton, SO17 1BJ, UK*
[f] *Istituto Nazionale di Fisica Nucleare, Sezione di Roma Tre, Italy*

E-mail: silvano.simula@roma3.infn.it

We present the comparison of existing experimental data for the radiative leptonic decays $P \to \ell\nu_\ell\gamma$, where $P = K$ or π and $\ell = e$ or μ, from the KLOE, PIBETA, E787, ISTRA+ and OKA collaborations with the theoretical predictions based on the recent non-perturbative determinations of the structure-dependent vector and axial-vector form factors, F_V and F_A respectively. These were obtained using lattice QCD+QED simulations at order $O(\alpha_{\rm em})$ in the electromagnetic coupling. We find good agreement with the KLOE data on $K \to e\nu_e\gamma$ decays from which the form factor $F^+ = F_V + F_A$ can be determined. For $K \to \mu\nu_\mu\gamma$ decays we observe differences of up to 3 - 4 standard deviations at large photon energies between the theoretical predictions and the data from the E787, ISTRA+ and OKA experiments and similar discrepancies in some kinematical regions with the PIBETA experiment on radiative pion decays. A global study of all the kaon-decay data within the Standard Model results in a poor fit, largely because at large photon energies the KLOE and E787 data cannot be reproduced simultaneously in terms of the same form factor F^+. The discrepancy between the theoretical and experimental values of the form factor $F^- = F_V - F_A$ is even more pronounced. These observations motivate future improvements of both the theoretical and experimental determinations of the structure-dependent form factors F^+ and F^-, as well as further theoretical investigations of models of "new physics" which might for example, include possible flavor changing interactions beyond $V - A$ and/or non-universal corrections to the lepton couplings.

The 38th International Symposium on Lattice Field Theory, LATTICE2021 26th-30th July, 2021 Zoom/Gather@Massachusetts Institute of Technology

*Speaker

PoS(LATTICE2021)631

1. Introduction

The decays of charged pseudoscalar mesons into light leptons, $P \to \ell\nu_\ell[\gamma]$ where ℓ stands for an electron or a muon, represent an important contribution to flavor physics since they give access to fundamental parameters of the Standard Model (SM), in particular to the Cabibbo-Kobayashi-Maskawa (CKM) matrix elements [1]. At tree level, i.e. without a photon in the final state, these decays are helicity suppressed in the SM due to the $V-A$ structure of the leptonic weak charged current, while the helicity suppression can be overcome by the radiated photons. Therefore, radiative leptonic decays may provide sensitive probes of possible SM extensions inducing non-standard currents and/or non-universal corrections to the lepton couplings.

Radiative leptonic decays also provide a powerful tool with which to investigate the internal structure of the decaying meson. In addition to the leptonic decay constant f_P, there are other structure-dependent (SD) amplitudes describing the emission of real photons from hadronic states, usually parameterized in terms of the vector F_V and axial-vector F_A form factors. Thus, a first-principle calculation of radiative leptonic decays requires a non-perturbative accuracy, which can be provided by numerical QCD+QED simulations on the lattice.

In Ref. [2] a strategy was proposed to enable lattice computations of QED radiative corrections to $P^+ \to \ell^+\nu_\ell[\gamma]$ decay rates at order $O(\alpha_{\rm em})$. The strategy naturally obeys the Bloch-Nordsieck mechanism [3], in which the cancellation of infrared divergences occurs between contributions to the rate with real photons in the final state and those with virtual photons in the decay amplitude.

Within the RM123 expansion framework [4, 5] the strategy of Ref. [2] was applied in Refs. [6, 7] to provide the first non-perturbative calculation of the SD virtual contribution to the pion and kaon decay rates into muons. The contribution with a real photon in the final state was evaluated non-perturbatively in Ref. [8] by performing numerical lattice QCD+QED simulations at order $O(\alpha_{\rm em})$ in the electroquenched approximation, in which the sea quarks are electrically neutral.

In this contribution we present the comparison carried out in detail in Ref. [9] between the theoretical predictions based on the non-perturbative determination of the SD form factors F_V and F_A evaluated in Ref. [8] and the experimental data available on the leptonic radiative decay $K \to e\nu_e\gamma$ from the KLOE Collaboration [10], on the decay $K \to \mu\nu_\mu\gamma$ from E787 [12], ISTRA+ [14] and OKA [15] collaborations and on the decay $\pi^+ \to e^+\nu_e\gamma$ from the PIBETA Collaboration [16].

2. Differential rates for radiative leptonic decays

Following Refs. [2, 8] the double differential rate for the radiative leptonic decay of a charged pseudoscalar meson, $P^+ \to \ell^+\nu_\ell\gamma$, can be written as the sum of the five contributions:

$$\frac{d^2\Gamma(P^+ \to \ell^+\nu_\ell\gamma)}{dx_\gamma dx_\ell} = \frac{\alpha_{\rm em}}{4\pi}\Gamma^{(0)} \left[\frac{d^2R_1^{\rm pt}}{dx_\gamma dx_\ell} + \frac{d^2R_1^{\rm SD^-}}{dx_\gamma dx_\ell} + \frac{d^2R_1^{\rm SD^+}}{dx_\gamma dx_\ell} + \frac{d^2R_1^{\rm INT^-}}{dx_\gamma dx_\ell} + \frac{d^2R_1^{\rm INT^+}}{dx_\gamma dx_\ell} \right], \qquad (1)$$

where the subscript 1 denotes the number of photons in the final state, while x_γ and x_ℓ are the photon and lepton kinematical variables, defined as $x_\gamma \equiv (2P\cdot k)/m_P^2$ and $x_\ell \equiv (2P\cdot p_\ell)/m_P^2 - r_\ell^2$, where P is the four-momentum of the decaying meson with mass m_P, p_ℓ is the four-momentum of the final-state lepton with mass m_ℓ, k is the four-momentum of the photon and $r_\ell \equiv m_\ell/m_P$. In the rest frame of the decaying meson one has $x_\gamma = 2E_\gamma/m_P$ and $x_\ell = 2E_\ell/m_P - r_\ell^2$, where E_γ and E_ℓ

are the photon and lepton energies respectively. In Eq. (1) the quantity $\Gamma^{(0)}$ is the leptonic decay rate at tree level, given explicitly by $\Gamma^{(0)} = G_F^2 |V_{\rm CKM}|^2 f_P^2 m_P^3 r_\ell^2 \left(1 - r_\ell^2\right)^2 / (8\pi)$, where G_F is the Fermi constant, $V_{\rm CKM}$ the relevant CKM matrix element and f_P the leptonic decay constant of the P-meson. The other entries on the right-hand side of Eq. (1) are

$$d^2R_1^{\rm pt}/dx_\gamma dx_\ell = 2 f_{\rm pt}(x_\gamma, x_\ell)/(1 - r_\ell^2)^2 \,, \tag{2}$$

$$d^2R_1^{\rm SD^\pm}/dx_\gamma dx_\ell = m_P^2 f_{\rm SD}^\pm(x_\gamma, x_\ell) \left[F^\pm(x_\gamma)\right]^2 / 2 f_P^2 r_\ell^2 (1 - r_\ell^2)^2 \,, \tag{3}$$

$$d^2R_1^{\rm INT^\pm}/dx_\gamma dx_\ell = -2 m_P f_{\rm INT}^\pm(x_\gamma, x_\ell) F^\pm(x_\gamma) / f_P \, (1 - r_\ell^2)^2 \,, \tag{4}$$

where the superscripts $\pm$ correspond to the photon helicities and the three terms in Eqs. (2)-(4) represent respectively the contribution of the point-like (pt) approximation of the decaying meson, the SD contribution and the contribution from the interference (INT) between the pt and SD terms. Note that in the literature the pt contribution is often referred to as the inner-bremsstrahlung term. The kinematical functions appearing in Eqs. (2)-(4) can be read off from Ref. [9], while the quantities $F^\pm(x_\gamma) \equiv F_V(x_\gamma) \pm F_A(x_\gamma)$ are the SD form factors in the photon helicity basis.

Recently the SD form factors have been determined on the lattice for decaying pions, kaons, D and D_s mesons for a wide range of values of x_γ [8]. For pion and kaon decays ($P = \pi, K$) we make use of the linear parameterization of the physical results for F_V and F_A given in Section V of Ref. [8], which reproduces our lattice data throughout the physical region, i.e. we write

$$F_V^P(x_\gamma) = C_V^P + D_V^P x_\gamma \,, \qquad F_A^P(x_\gamma) = C_A^P + D_A^P x_\gamma \tag{5}$$

where the parameters $C_{V(A)}^P$ and $D_{V(A)}^P$, including their correlations, can be read off from Ref. [9]. In the following the uncertainties and correlations of the two form factors are taken into account adopting multivariate gaussian distributions with 10,000 events. We will compare our results also with the ChPT predictions at order $O(e^2p^4)$, based on the following x_γ-independent form factors

$$C_V^{\rm ChPT} = m_P/4\pi^2 f_P \,, \quad D_V^{\rm ChPT} = 0 \,, \qquad C_A^{\rm ChPT} = 8 m_P (L_9^r + L_{10}^r)/f_P \,, \quad D_A^{\rm ChPT} = 0 \tag{6}$$

with $L_9^r + L_{10}^r = 0.0017\,(7)$ [17], $m_\pi/f_\pi = 139.6$ MeV/130.4 MeV and $m_K/f_K = 493.7$ MeV/156.1 MeV.

3. Comparison with the experimental data

The experimental data from the KLOE, E787, ISTRA+, OKA and PIBETA collaborations [10, 12, 14–16] correspond to radiative decay rates integrated over the lepton variable x_ℓ and including specific kinematical cuts on the lepton momentum and/or on the emission angle $\theta_{\ell\gamma}$ between the lepton and the photon. The way the specific experimental cuts are taken into account in the theoretical predictions is described in Ref. [9] for each experiment.

3.1 The KLOE experiment

In Ref. [10] the KLOE Collaboration has measured the differential decay rate $d\Gamma(K_{e2\gamma})/dE_\gamma$ for photon energies in the range 10 MeV $< E_\gamma < E_\gamma^{max} \simeq 250$ MeV with the constraint $p_e > 200$ MeV, adopting five different bins of photon energies, namely

$$\Delta R^{{\rm exp},i} \equiv \int_{E_\gamma^i}^{E_\gamma^{i+1}} dE_\gamma \, \frac{1}{\Gamma(K_{\mu 2[\gamma]})} \left[\frac{d\Gamma(K_{e2\gamma})}{dE_\gamma}\right]_{p_e > 200{\rm MeV}} \tag{7}$$

with $E_\gamma^i = \{10, 50, 100, 150, 200, 250\}$ MeV.

Using our lattice form factors (5) we have computed the theoretical predictions $\Delta R^{\mathrm{th},i}$ for each bin. The INT contributions turn out to be totally negligible ($\lesssim 10^{-10}$), while the pt term only contributes significantly in the first bin (10 MeV $< E_\gamma <$ 50 MeV) where however, it is the dominant contribution leading therefore to a precise prediction for this bin. For the remaining 4 bins our predictions $\Delta R^{\mathrm{th},i}$ are largely dominated by the SD$^+$ contribution related to $[F^+(x_\gamma)]^2$. Our results are shown in the left panel of Fig. 1 together with the experimental data $\Delta R^{\mathrm{exp},i}$ from KLOE and the ChPT predictions at order $O(e^2p^4)$ (see Eq. (6) with $m_K/f_K = 493.7\,\mathrm{MeV}/156.1\,\mathrm{MeV}$). For all bins a consistency between theory and experiment is observed within ≈ 1 standard deviation. This consistency is underlined in the right panel of Fig. 1, where we compare the form factor $F^+(x_\gamma)$ extracted by the KLOE collaboration in Ref. [10] with our theoretical predictions.

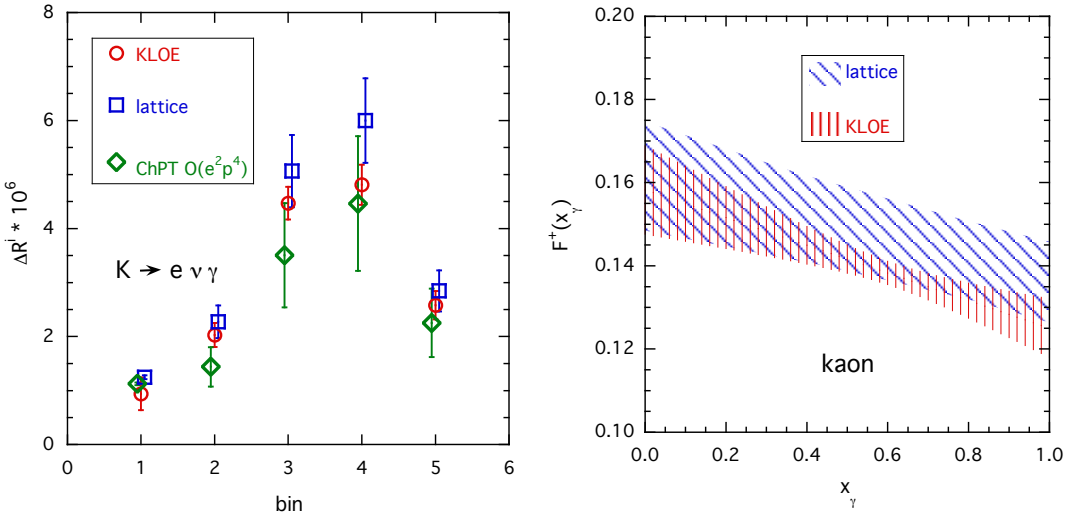

Figure 1: *Left panel: comparison of the KLOE experimental data $\Delta R^{\mathrm{exp},i}$ [10] (red circles) with the theoretical predictions $\Delta R^{\mathrm{th},i}$ (blue squares), evaluated with the SD form factors of Ref. [8] given in Eq. (5). The green diamonds correspond to the prediction of ChPT at order $O(e^2p^4)$, based on the SD form factors (6). Right panel: Comparison of the form factor $F^+(x_\gamma)$ extracted by the KLOE collaboration in Ref. [10] and our theoretical prediction (5). The shaded areas represent uncertainties at the level of 1 standard deviation.*

The KLOE collaboration has also determined the total branching ratio corresponding to the sum over the five photon energy bins of the experiment [10], namely to $E_\gamma > 10$ MeV with the kinematical cut $p_e > 200$ MeV:

$$\Delta R^{\mathrm{exp}}\left(E_\gamma > 10\,\mathrm{MeV}, p_e > 200\,\mathrm{MeV}\right) \equiv \sum_{i=1}^{5} \Delta R^{\mathrm{exp},i}\,. \tag{8}$$

The same quantity has been measured recently by the J-PARC E36 collaboration [11]. The two measurements are shown in Table 1 and compared with our lattice prediction [9] and the one from ChPT at order $O(e^2p^4)$. It can be seen that the two experimental results differ by ≈ 2.5 standard deviations. Our lattice prediction is consistent with both J-PARC and KLOE measurements (within 0.4 and 1.2 standard deviations, respectively) due to the present larger theoretical uncertainty.

E_γ (MeV)	p_e (MeV)	KLOE [10]	J-PARC E36 [11]	lattice [9]	ChPT
10 - 250	> 200	$1.483 \pm 0.066 \pm 0.013$	$1.85 \pm 0.11 \pm 0.07$	1.743 ± 0.212	1.279 ± 0.324

Table 1: *Values of the branching ratio $\Delta R^{\rm exp}$, in units of 10^{-5}, measured by the KLOE [10] and J-PARC E36 [11] experiments corresponding to $E_\gamma > 10$ MeV with the kinematical cut $p_e > 200$ MeV. In the third and fourth columns the first error is statistical and the second one is systematic. The experimental findings are compared with our lattice prediction [9], evaluated with the vector and axial form factors of Ref. [8] given in Eq. (5), and with the prediction of ChPT at order $O(e^2p^4)$, based on the vector and axial form factors given in Eq. (6).*

3.2 The E787 experiment

In Ref. [12] the E787 Collaboration has investigated the $K_{\mu 2\gamma}$ decay for photon energies in the range $90\,\text{MeV} < E_\gamma < E_\gamma^{max} \simeq 235\,\text{MeV}$ with the constraint that the muon kinetic energy is larger than 137 MeV (i.e. $E_\mu > m_\mu + 137\,\text{MeV} \simeq 243\,\text{MeV}$). In such kinematical regions the radiated photons come mainly from the pt contribution and the SD^+ terms [12]. In order to compare their results with those from other experiments, the E787 data are integrated over the small allowed range of muon energies $243\,\text{MeV} < E_\mu \leq E_\mu^{max} \simeq 258\,\text{MeV}$, assuming a constant acceptance, to obtain the differential branching ratio

$$\frac{dR^{\rm exp}}{d\cos(\theta_{\mu\gamma})} = \frac{1}{\Gamma(K_{\mu 2[\gamma]})}\left[\frac{d\Gamma(K_{\mu 2\gamma})}{d\cos(\theta_{\mu\gamma})}\right]_{E_\gamma > 90\,\text{MeV}, E_\mu > 243\,\text{MeV}} \tag{9}$$

as a function of the emission angle $\theta_{\mu\gamma}$ between the muon and the photon in the kaon rest-frame.

Since the pt contribution is a purely kinematical factor, it can be subtracted from the experimental data without introducing any uncertainty. The corresponding *subtracted* data are compared with our theoretical predictions in Fig. 2. A reasonable agreement is found except for some points at large backward angles, i.e. at large photon energies, where the tension reaches about 2 - 3 standard deviations. There the data are dominated by the contributions coming from the form factor $F^+(x_\gamma)$. Note that, though generally small, the relative contribution of SD^-+INT^-, which depends on the form factor $F^-(x_\gamma)$, becomes more important as $\cos(\theta_{\mu\gamma})$ increases (i.e. as x_γ decreases), reaching about 20 - 30% of the term SD^++INT^+ at the lowest available values of x_γ.

We remind that our lattice form factor $F^+(x_\gamma)$ leads to a good description of the KLOE data [10] (see Sec. 3.1). Thus, the tension between our theoretical predictions and the E787 data, visible at large x_γ in Fig. 2, is not unexpected. The KLOE collaboration has estimated $F^+(x_\gamma = 1)$ to be equal to $0.125 \pm 0.007_{\rm stat} \pm 0.001_{\rm syst}$ [10], while the estimate of E787, assuming a constant form factor, is $0.165 \pm 0.007_{\rm stat} \pm 0.011_{\rm syst}$ [12]. The difference is at the level of about 3 standard deviations. Our theoretical prediction for this quantity is $F^+(x_\gamma = 1) = 0.1362 \pm 0.0096$.

Thus, further experimental investigations of the form factor $F^+(x_\gamma)$ in radiative kaon decays into electrons and muons are required. In particular, an investigation of the decay $K_{e2\gamma}$ at large electron energies will provide the opportunity for an accurate determination of $|F^+(x_\gamma)|$ for a wide range of values of x_γ. This is illustrated in Fig. 3, where the pt, SD^+, SD^-, INT^+ and INT^-

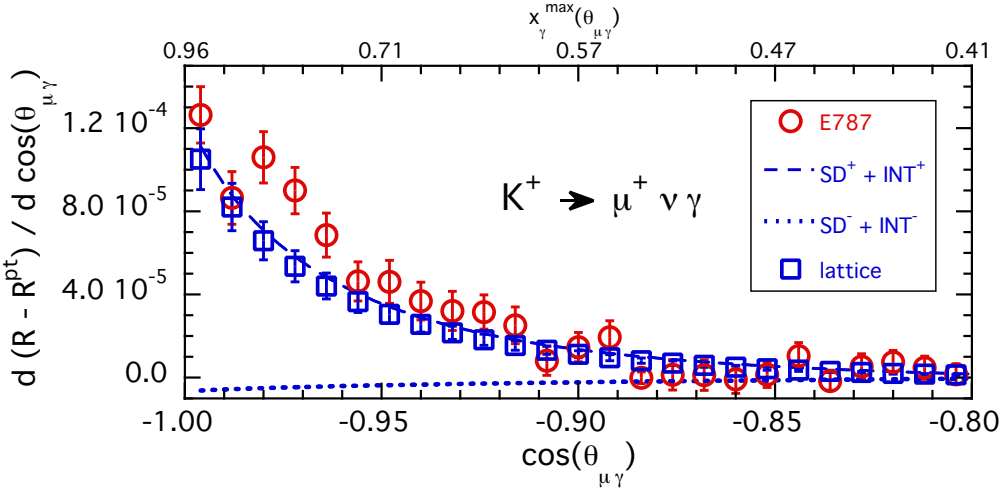

Figure 2: *Comparison of the E787 experimental data after the pt contribution has been subtracted, $d(R^{\rm exp} - R^{\rm pt})/d\cos(\theta_{\mu\gamma})$ (red circles) [12], with the theoretical predictions $d(R^{\rm th} - R^{\rm pt})/d\cos(\theta_{\mu\gamma})$ (blue squares), evaluated using the lattice form factors of Ref. [8] given in Eq. (5). The dashed and dotted lines correspond to the theoretical contributions $d(R^{\rm SD^+} + R^{\rm INT^+})/d\cos(\theta_{\mu\gamma})$ and $d(R^{\rm SD^-} + R^{\rm INT^-})/d\cos(\theta_{\mu\gamma})$ respectively. The upper horizontal axis shows the maximum value of x_γ, $x_\gamma^{max}(\theta_{\mu\gamma})$, allowed by the value of the angle $\theta_{\mu\gamma}$ taking into account the kinematical cuts of the E787 experiment.*

contributions to the differential branching ratio

$$\frac{dR}{d\cos(\theta_{e\gamma})} = \frac{1}{\Gamma(K_{e2[\gamma]})}\left[\frac{d\Gamma(K_{e2\gamma})}{d\cos(\theta_{e\gamma})}\right]_{x_\gamma>0.2,\, x_e>0.93} \tag{10}$$

are shown as a function of the emission angle $\theta_{e\gamma}$ between the electron and the photon (in the kaon rest-frame) after considering the kinematical cuts $x_\gamma > 0.2$ ($E_\gamma > 49$ MeV) and $x_e > 0.93$ ($E_e > 230$ MeV). These kinematical cuts are indicative of a possible definition of a signal region with minimal background contamination both from the pt contribution to $K_{e2\gamma}$ and from the semileptonic K_{e3} process in a fixed-target forward detector such as that in the NA62 experiment [13].

3.3 The ISTRA+ and OKA experiments

In Refs. [14] and [15] the ISTRA+ and OKA collaborations have selected appropriate kinematical regions (strips) in order to determine the contribution of the interference term INT$^-$. For each strip, specific bins are selected in the photon and muon variables x_γ and $y_\mu \equiv 2E_\mu/m_K = x_\mu + r_\mu^2$, where E_μ is the muon energy in the kaon rest frame. A further constraint $\cos(\theta_{\mu\gamma}) > \cos(\theta_{\rm cut})$ is imposed on the emission angle $\theta_{\mu\gamma}$ between the muon and the photon. In both experiments the measured observable is the ratio $N_{\rm exp}/N_{\rm pt}$ of the number of observed photons in each strip to the number of pt (or inner-bremsstrahlung) events. $N_{\rm pt}$ is estimated using the Geant3 package [18].

The comparison of the experimental results with our predictions, and also with those obtained using ChPT at order $O(e^2p^4)$ (see Eq. (6) with $m_K/f_K = 493.7$ MeV$/156.1$ MeV) is presented in Fig. 4. It can clearly be seen that at large photon energies there is a significant tension between the experimental data and our non-perturbative results (and also those obtained using ChPT). Thus, improved determinations of the form factor $F^-(x_\gamma)$ are required from both experiment and theory in order to consolidate or eliminate the discrepancies.

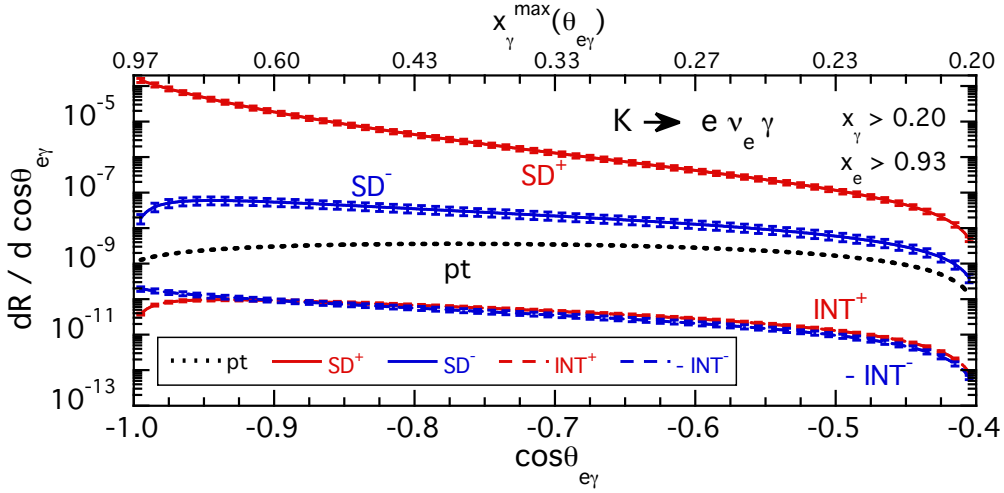

Figure 3: *Results for the pt, SD^+, SD^-, INT^+ and INT^- contributions to the differential branching ratio (10) as a function of the emission angle $\theta_{e\gamma}$ for the decay process $K_{e2\gamma}$, calculated using the lattice form factors of Ref. [8], given in Eq. (5), with the kinematical cuts $x_\gamma > 0.2$ ($E_\gamma > 49$ MeV) and $x_e > 0.93$ ($E_e > 230$ MeV).*

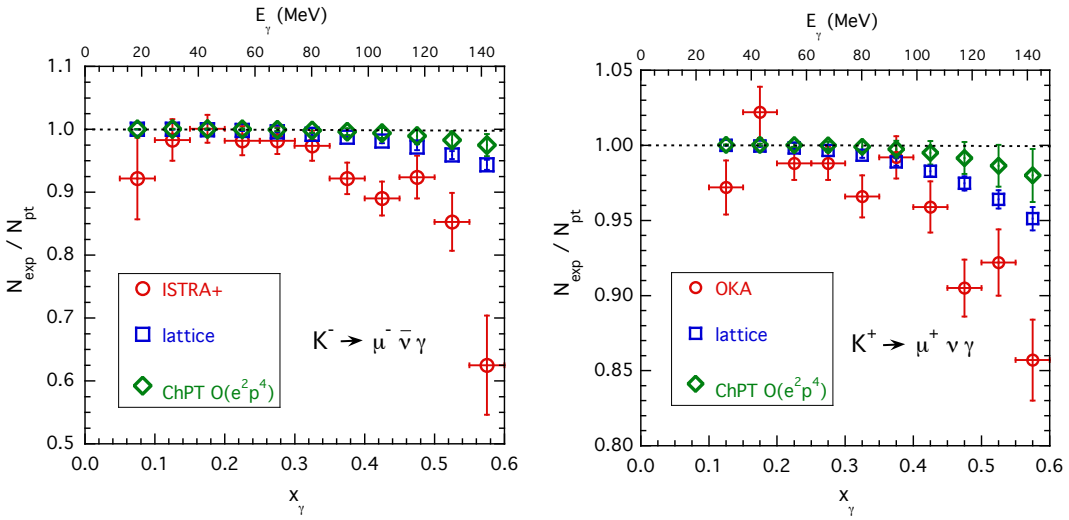

Figure 4: *Comparison of the experimental results from the ISTRA+ [14] (left panel) and OKA [15] (right panel) collaborations with our theoretical predictions, based on the form factors of Ref. [8], given in Eq. (5). The green diamonds correspond to the ChPT prediction at order $O(e^2p^4)$, based on the form factors (6). Note the different scales of the vertical axes in the two panels.*

3.4 The PIBETA experiment

In Ref. [16] the PIBETA Collaboration has investigated the radiative pion decay into electrons $\pi_{e2\gamma}$ and has measured the following branching ratios

$$\Delta R^{\mathrm{exp},i} \equiv \frac{1}{\Gamma(\pi \to \mu\nu[\gamma])} \int_{E_\gamma^i}^{E_\gamma^{max}} dE_\gamma \int_{E_e^i}^{E_e^{max}} dE_e \left[\frac{d^2\Gamma(\pi^+ \to e^+\nu\gamma)}{dE_\gamma dE_e}\right]_{\theta_{e\gamma}>40^\circ} \tag{11}$$

integrated in four different kinematical regions of photon and electron energies with the constraint $\theta_{e\gamma} > 40^\circ$. The kinematical regions are labelled as $i = A, B, C, O$ and the values of

the minimum photon and electron energies are, respectively, $E_\gamma^i = \{50, 50, 10, 10\}$ MeV and $E_e^i = \{50, 10, 50, m_e\}$ MeV. The maximum photon and electron energies are $E_\gamma^{max} \simeq E_e^{max} \simeq m_\pi/2 \simeq 70$ MeV. The region O is a combination of the other three regions supplemented with extrapolations based on Monte Carlo simulations [16].

Using the form factors (5) we have evaluated the theoretical prediction $\Delta R^{\mathrm{th},i}$ for each kinematical region. The INT contribution is negligible in all the kinematical regions and the SD term is dominant only in region A, while in the other kinematical regions the pt term dominates. Thus, in order to better highlight the SD term we subtract from the experimental data the pt contribution, which is known precisely. The values of $\Delta R^{\mathrm{pt},i}$, of our non-perturbative predictions for $\Delta R^{\mathrm{th},i} - \Delta R^{\mathrm{pt},i}$ and of the *subtracted* experimental data $\Delta R^{\mathrm{exp},i} - \Delta R^{\mathrm{pt},i}$ are shown in Fig. 5 together with the ChPT predictions at order $O(e^2p^4)$, based on the form factors (6) with $m_\pi/f_\pi = 139.6$ MeV/130.4 MeV.

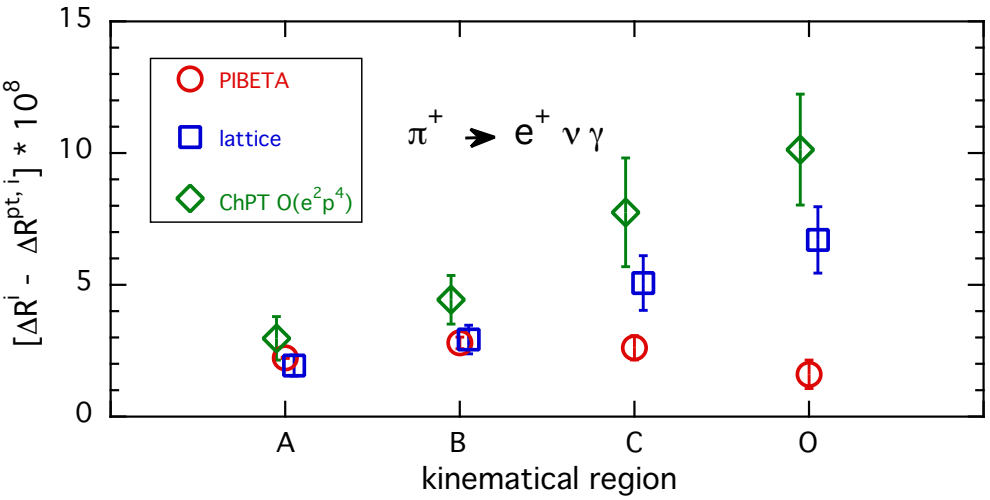

Figure 5: *Comparison of the PIBETA experimental data [16] after the subtraction of the pt contribution, $(\Delta R^{\mathrm{exp},i} - \Delta R^{\mathrm{pt},i})$ (red circles), with the theoretical predictions $(\Delta R^{\mathrm{th},i} - \Delta R^{\mathrm{pt},i})$ (blue squares), evaluated with the form factors of Ref. [8] given in Eq. (5), for the four kinematical regions of the PIBETA experiment. The green diamonds correspond to the ChPT prediction at order $O(e^2p^4)$, based on the form factors (6).*

It can be seen that in the kinematical regions A and B the agreement between theory and experiment is good, while for the kinematical regions C and O, where the ChPT predictions at order $O(e^2p^4)$ also differ significantly from the measurements, a tension occurs at a level of about 2.2 and 4.1 standard deviations respectively.

4. SM fit to the experimental data

The results obtained in the previous sections naturally raise the issue of whether the SD form factors can be modified in such a way as to significantly reduce the discrepancies with all the experimental data while staying within the SM. To this end the KLOE, E787, ISTRA+ and OKA data can be fitted simultaneously since they concern kaon decays, while only the PIBETA experiment measures the pion decay rates. We stress that the discussion in this section assumes the validity of the SM in general, and lepton-flavour universality in particular, allowing us to combine data from kaon decays into electrons and muons.

In fitting the kaon data we adopt a simple linear parameterization of the form factors $F_\pm(x_\gamma)$, suggested by our lattice results, namely

$$F_\pm(x_\gamma) = \widetilde{C}_\pm + \widetilde{D}_\pm x_\gamma \ , \tag{12}$$

where the four quantities $\widetilde{C}_\pm$ and $\widetilde{D}_\pm$ are now treated as free parameters.

A total of 51 experimental data points (5 points from KLOE, 25 points from E787, 11 points from ISTRA+ and 10 points from OKA) are fitted using the form factors (12) adopting a standard χ^2-minimization procedure with a bootstrap sample of 5000 events generated to propagate the uncertainties of the experimental data and giving the same weight to each of the four experiments. In our fitting procedure the experimental data are treated as uncorrelated, since no correlation matrix is available. The quality of the best fit is poor: the optimal value of χ^2/(no. of points) is equal to 1.3, 5.3, 3.1 and 2.2 for the KLOE, E787, ISTRA+ and OKA data, respectively. The comparison of the results of the global SM fit with all the experimental data is shown in Fig. 6. The largest tension occurs for the E787 data and is a consequence of the simultaneous presence of the KLOE data.

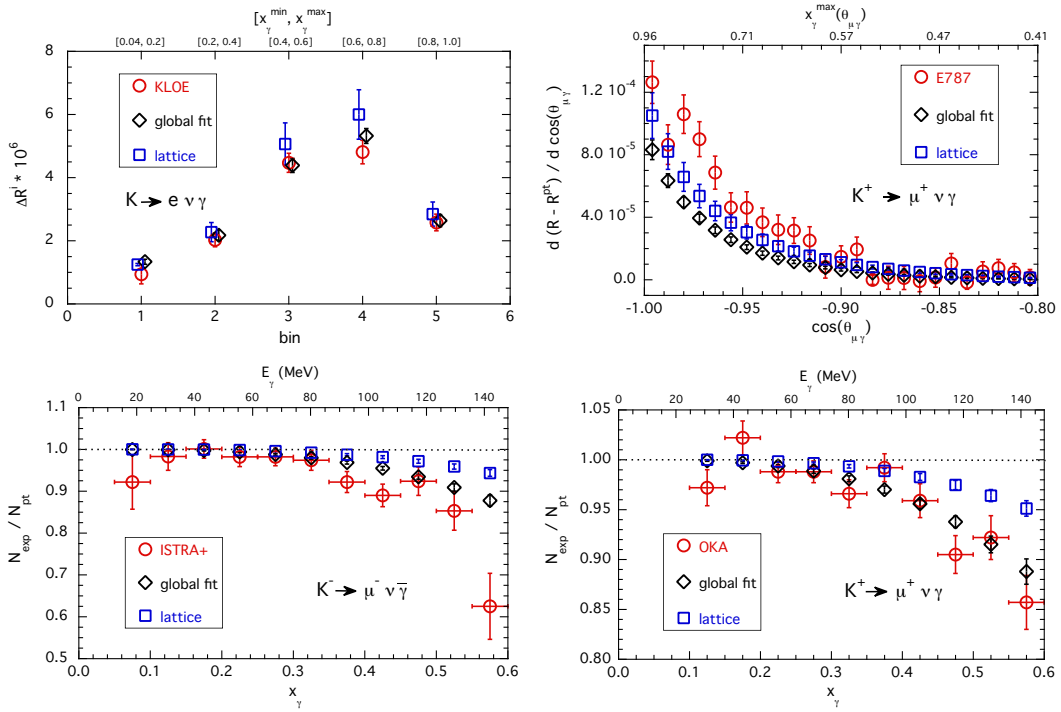

Figure 6: *Results of the global SM fit (black diamonds) applied to the KLOE [10], E787 [12], ISTRA+ [14] and OKA [15] data (red circles) adopting the linear parameterization (12) for the form factors $F^\pm(x_\gamma)$. The blue squares represent the SM predictions evaluated with the lattice form factors determined in Ref. [8].*

In Fig. 7 the "optimal" form factors, obtained from Eq. (12), are compared to our lattice form factors, obtained from Eq. (5), and to the predictions of ChPT at order $O(e^2p^4)$ given by Eq. (6). While the discrepancy for the form factor $F^+(x_\gamma)$ is relatively mild, for $F^-(x_\gamma)$ there is a discrepancy of a factor of ≈ 2 with the lattice results and even more with the $O(e^2p^4)$ ChPT predictions.

Our findings call for improvements in the determination of the SD form factors $F^\pm(x_\gamma)$ from both experiment and theory. In this respect, we look forward to the results from the analysis of the

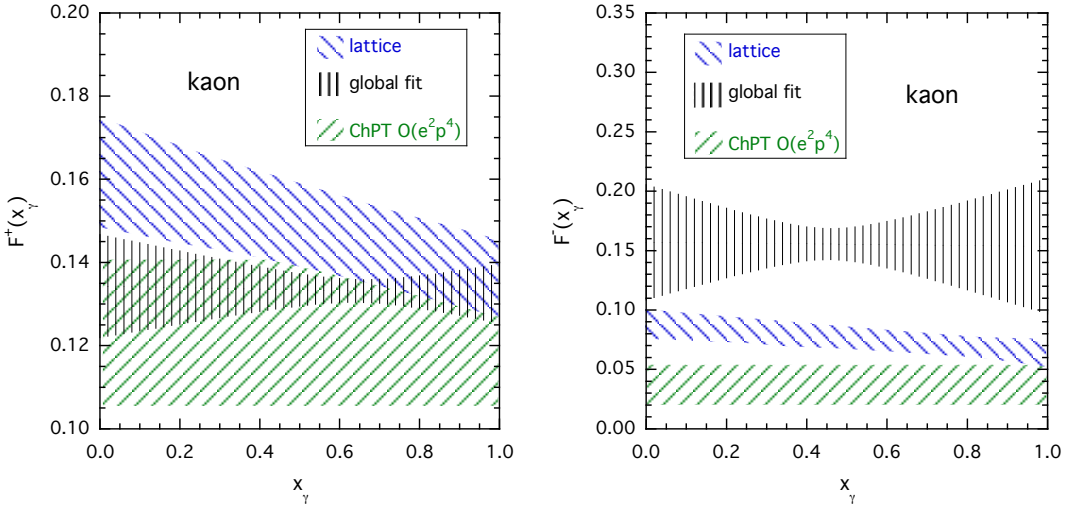

Figure 7: *Comparison of the form factors $F^+(x_\gamma)$ (left panel) and $F^-(x_\gamma)$ (right panel), obtained by the simultaneous fit (12) of the KLOE [10], E787 [12], ISTRA+ [14] and OKA [15] experimental data, with our lattice results from Ref. [8] corresponding to Eq. (5) and with the ChPT predictions at order $O(e^2p^4)$ given by Eq. (6). All the shaded areas represent uncertainties at the level of 1 standard deviation.*

NA62 experiment on the $K_{e2\gamma}$ decay, which is in progress and is expected to provide the most precise determination of $|F^+(x_\gamma)|$ [13]. If a discrepancy between the form factors obtained from decays into electrons from NA62 and those obtained from decays into muons from the E787 experiment will be confirmed, this would provide a motivation for better determinations also of the form factors from $K \to \mu\nu_\mu\gamma$ decays. On the theoretical side it can be expected that the precision achieved in Ref. [8] will be improved in the next generation of computations.

We point out that it is also conceivable that the tensions observed above between the experimental data and our lattice predictions are due to the presence of new physics, such as flavor changing interactions beyond the $V-A$ couplings of the Standard Model and/or non-universal corrections to the lepton couplings. This possibility deserves further theoretical investigations.

Acknowledgments

We gratefully acknowledge discussions with members of the experimental collaborations about their data and results and we thank in particular B. Sciascia and T. Spadaro from KLOE [10], M.R. Convery from E787 [12] and M. Bychkov from PIBETA [16]. We also thank V. Kravtsov, V. Duk and V. Obraztsov for supplying us with the kinematical cuts of the OKA experiment [15] and A. Romano for discussions about the status of the ongoing analysis by the NA62 experiment. We acknowledge PRACE for awarding us access to Marconi at CINECA under the grant Pra17-4394 and CINECA for the provision of CPU time under the specific initiative INFN-LQCD123. C.T.S. was partially supported by an Emeritus Fellowship from the Leverhulme Trust and by STFC (UK) grants ST/P000711/1 and ST/T000775/1. N.T. and R.F. acknowledge the University of Rome Tor Vergata for the support granted to the project PLNUGAMMA. F.S. and S.S. are supported by MIUR under grant PRIN 20172LNEEZ. F.S. is supported by INFN under GRANT73/CALAT.

References

[1] P. A. Zyla *et al.* [Particle Data Group], PTEP **2020** (2020) no.8, 083C01

[2] N. Carrasco *et al.*, Phys. Rev. D **91** (2015) no.7, 074506 [arXiv:1502.00257 [hep-lat]].

[3] F. Bloch and A. Nordsieck, Phys. Rev. **52** (1937) 54.

[4] G.M. de Divitiis *et al.*, JHEP **1204** (2012) 124 [arXiv:1110.6294 [hep-lat]].

[5] G.M. de Divitiis *et al.*, Phys. Rev. D **87** (2013) no.11, 114505 [arXiv:1303.4896 [hep-lat]].

[6] D. Giusti *et al.*, Phys. Rev. Lett. **120** (2018) no.7, 072001 [arXiv:1711.06537 [hep-lat]].

[7] M. Di Carlo *et al.*, Phys. Rev. D **100** (2019) no.3, 034514 [arXiv:1904.08731 [hep-lat]].

[8] A. Desiderio *et al.* Phys. Rev. D **103** (2021) no.1, 014502 [arXiv:2006.05358 [hep-lat]].

[9] R. Frezzotti *et al.*, Phys. Rev. D **103** (2021) no.5, 053005 [arXiv:2012.02120 [hep-ph]].

[10] F. Ambrosino *et al.* [KLOE], Eur. Phys. J. C **64** (2009), 627-636 [arXiv:0907.3594 [hep-ex]].

[11] H. Ito *et al.* [J-PARC E36] [arXiv:2107.03583 [hep-ex]].

[12] S. Adler *et al.* [E787], Phys. Rev. Lett. **85** (2000), 2256-2259 [arXiv:hep-ex/0003019 [hep-ex]].

[13] A. Romano [for the NA62 Collaboration], private communication.

[14] V. Duk *et al.* [ISTRA+], Phys. Lett. B **695** (2011), 59-66 [arXiv:1005.3517 [hep-ex]].

[15] V. Kravtsov *et al.* [OKA], Eur. Phys. J. C **79** (2019) no.7, 635 [arXiv:1904.10078 [hep-ex]].

[16] M. Bychkov *et al.*, Phys. Rev. Lett. **103** (2009), 051802 [arXiv:0804.1815 [hep-ex]].

[17] J. Bijnens and G. Ecker, Ann. Rev. Nucl. Part. Sci. **64** (2014), 149 [arXiv:1405.6488 [hep-ph]].

[18] R. Brun, F. Bruyant, M. Maire, A.C. McPherson and P. Zanarini, CERN-DD/EE/84-1 (1987).